Controlling the structural transition at the Néel point of CrN epitaxial thin films using epitaxial growth

Kei Inumaru, Kunihiko Koyama, Naoya Imo-oka, and Shoji Yamanaka
Department of Applied Chemistry, Graduate School of Engineering, Hiroshima University, 1-4-1, Kagamiyama, Higashi-Hiroshima, Hiroshima 739-8527, Japan

(Received 5 October 2006; revised manuscript received 11 December 2006; published 22 February 2007)

Chromium nitride (CrN) films were epitaxially grown on α-Al_2O_3(0001) and MgO (001) substrates by pulsed laser deposition at 973 K under nitrogen radical irradiation, and the structural change of the films was investigated at around the Néel temperature of CrN (~270 K) by temperature-controlled x-ray diffraction experiments. Bulk cubic CrN is known to show monoclinic distortion below the Néel temperature. The CrN film grown on MgO(001) with the CrN(001) plane parallel to the substrate surface, exhibited a clear structural change at around 260 K. On the other hand, on α-Al_2O_3(0001) substrates, the CrN phase grew with its (111) planes parallel to the substrate surface, and showed no structural change at the Néel temperature. The different orientation of the epitaxial films can explain the different behavior of the films: The structural transition of bulk-CrN causes large variations in the interatomic distances and bond angles on the (111) plane, but varies little on the (001) plane. In the case of thin films, the α-Al_2O_3(0001) substrate surface could prevent the (111)-oriented film from distorting its structure by fixing atom positions on the CrN(111) interfaces of the film. In accordance with the structural behavior of the films, the (111)-oriented CrN film on α-Al_2O_3(0001) showed no anomaly in its metallic conductivity around the Néel temperature. On the other hand, the (001)-oriented CrN on MgO showed a steep increase in electrical conductivity, accompanied by a lattice distortion below the Néel point. These results highlight an example that epitaxy could be used to control the existence of structural transitions, further accompanied by an antiferromagnetic ordering, which is closely related to the electronic properties of materials.

DOI: 10.1103/PhysRevB.75.054416 PACS number(s): 74.78.−w, 81.15.Fg

INTRODUCTION

Lattice distortion often plays important roles in phenomena that are accompanied by drastic changes in the electronic structure and magnetic properties of the material studied. Recent topics are related to the interplay between lattice distortion and phenomena such as the charge/orbital ordering, which is characteristic of strongly correlated electron systems. A useful method to control lattice distortions is the heteroepitaxial growth of thin films on various substrates.[1–4] For example, anisotropic stress due to epitaxial growth induces the formation of a novel structure of orbital ordering in $Nd_{0.5}Sr_{0.5}MnO_3$ films on $SrTiO_3$ substrates.[1–3] The growth of manganite films on $SrTiO_3$ having different crystal orientation [(001), (011), and (111)], showed different first order phase transitions, further accompanied by the appearance of a novel orbital ordering. The strain in the epitaxial films had a large effect on the magnetism of the multilayer structure: the $La_{0.5}Ca_{0.5}MnO_3$ layer was sandwiched between two $Pr_{0.5}Ca_{0.5}MnO_3$ layers on $SrTiO_3$ (001), and the corresponding magnetic and transport properties were discussed in terms of the stabilized charge ordering and the vibration mode of the Jahn-Teller distortion.[5] Epitaxy also controls the lattice distortion and magnetism of elemental metals such as Mn (Refs. 6–8) and Cr.[9] The tetragonally distorted γ- and δ-Mn phases were stabilized by the epitaxial growth, and magnetism of these phases were strongly affected by the distortion. Epitaxy is also known to control the special inversion of the GaAs sublattice.[10]

Here, we report that the epitaxial growth of chromium nitride (CrN) can control the existence of structural transitions at the Néel temperature. The above-mentioned examples take advantage of epitaxy mainly to induce static strains. On the other hand, this report describes a method to allow or inhibit the structural transition of a material by controlling the orientation of the epitaxial growth: CrN films grown on MgO(001) exhibited a structural change at around its Néel temperature (ca 260 K). On the other hand, on α-Al_2O_3(0001) substrates, the CrN phase grew with its (111) planes parallel to the substrate surface, and showed no structural change at the Néel temperature. The electronic conductivity of the films showed behaviors in accordance with the controlled structural transition.

Antiferromagnetic compounds often exhibit lattice distortion at the Néel temperature. About fifty yeas ago, Corliss *et al.* revealed that CrN (NaCl-type structure) shows an antiferromagnetic transition at a Néel temperature of around 270 K.[11] Below the Néel temperature, CrN has a shear distortion consisting of a contraction in the angle α=90° to a value smaller by around 2°, the schematic illustration of which is presented in Fig. 1. The distorted structure forms double ferromagnetic layers alternately parallel to the [110] direction in such a way to form a four-layer antiferromagnetic orthorhombic unit cell. The detailed band calculations showed that the double layer antiferromagnetic ordering is slightly more favored over another single layered antiferromagnetic ordering, due to the stabilization effect of the lattice distortion.[12,13]

In contrast with the well-known structural and magnetic properties of CrN, the experimental studies reported different results on the electron transport properties of this material.[14–17] Some studies report that CrN is semiconducting,[14,16] while others report that the metallic conductivity of CrN is accompanied by a steep change around the

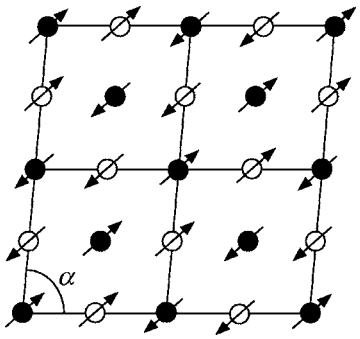

FIG. 1. Top view of CrN (001) plane in the Néel state. The distortion was exaggerated for clarity. Arrows denote the relative spin directions on Cr atoms. Solid and open circles represent Cr atoms with $z=0$ and $z=1/2$, respectively.

Néel temperature.[15,17] A recent study reported that the electronic conductivity of thin films changed from semiconducting to metallic behavior at around the Néel point when the film was cooled down.[17] In the present study, we compared the electron transport behaviors of CrN, both with and without the lattice distortion around and below the Néel point, and provide information on the correlation between the lattice distortion and the transport properties.

EXPERIMENTAL METHODS

The PLD system used in this study was equipped with a KrF excimer laser (COMPex102, Lambda Physics, Goettingen, Germany) and an rf-plasma radical source (model RF4.5, SVTA, MN, USA). The residual pressure of the chamber was less than 10^{-8} Torr. A Cr disk (99.9%) was used as the target. The oxide substrates were cleaned in methanol before their introduction into the vacuum chamber. Nitride films were deposited under irradiation of nitrogen radicals [RF power 350 W, N_2 feed 0.5 cm^3 (STP)/min]. We previously reported highly crystalline TiN,[18] CrN,[19] TiN-CrN multilayers,[20] Sr_2N,[21] $Ti_{1-x}Ni_xN_y$,[22] β-Mo_2N,[23] and NaCl-type MoN (B1-MoN) (Refs. 24 and 25) films prepared under radical irradiation. Before deposition, the substrates were irradiated with nitrogen radicals for around 15 min. The substrate temperature was 973 K and the pulse repetition rate was 20 Hz, and the power of the laser pulses was around 200 mJ. The film thickness and substrate used in the preparation of the films are listed in Table I. The crystal structures of the films were characterized by x-ray diffraction using two diffractometers. Conventional ω-2θ scans were performed with a D8 Advance diffractometer (Bruker AXS) using Cu K_α radiation with a Ni filter. The temperature-controlled x-ray diffraction patterns were measured using a TTA450 low temperature chamber (Anton Paar). The ω-2θ scans at variant Ψ angles were carried out with an XPert MRD diffractometer (Philips). The incident beam was a Cu K_α parallel beam from an x-ray mirror with a crossed slit (0.5 mm width and 5 mm height). The detector was equipped with a parallel-plate collimator and a Graphite monochromator (resolution, 0.27°). The nitrogen contents in the films were determined with an x-ray photoelectron spectrometer (Shimadzu ESCA-3400), which was calibrated with a standard CrN powder sample. Magnetic measurements were carried out with a magnetometer (Quantum Design MPMS-5S, USA). The thin film was placed parallel to the applied magnetic field. The film thickness was measured by atomic force microscopy (Nanoscope D-3100, Digital Instrument, USA) operated in tapping mode.

RESULTS AND DISCUSSION

Figure 2 shows the x-ray diffraction patterns (conventional ω-2θ scan) of the CrN films grown on MgO(001) (film A) and on α-Al_2O_3(0001) (film B). For film A, the CrN 002 diffraction was observed at $2\theta=43.42°$ at the higher angle side of the MgO 002 diffraction. The small peak at around 38.65° and the step observed at ca 41.47° are due to an incomplete removal of the CuK_β radiation and an artifact from the Ni filter, respectively. No other diffraction peak was observed except for those of MgO 004 and CrN 004, indicating that CrN grew with its (001) planes parallel to the substrate surface. On the other hand, for film B, with the exception of the peaks due to the α-Al_2O_3(0001) substrate, only peaks associated with CrN 111 at 37.02° and CrN 222 (not shown) were observed, demonstrating that CrN grew on α-Al_2O_3(0001) with its (111) planes parallel to the substrate surface. In order to obtain more information on the lattice

TABLE I. Structural parameters of thin films and bulk CrN. t_f: film thickness, rt: room temperature.

Sample	Substrate	Film orientation	t_f (nm)	Cell parameters				Ref.
				T (K)	a (nm)	c (nm)	α (°)	
Film A	MgO(001)	CrN(001)	86	rt	0.4135(2)	0.4177(2)	90	This work
Film B	α-Al_2O_3(0001)	CrN(111)	68	rt	0.4157(1)		89.32(4)	This work
Film C	α-Al_2O_3(0001)	CrN(111)	23	rt	0.4165(1)		89.72(4)	This work
CrN/MgO	MgO(001)	CrN(001)	89.4		0.406	0.413	90	Ref. 17
CrN/MgO	MgO(001)	CrN(001)	500	100		0.4178	90	Ref. 16
				300		0.4176	90	
bulk-CrN				77	0.4132	0.4134	88.32	Ref. 11
				rt	0.413		90	

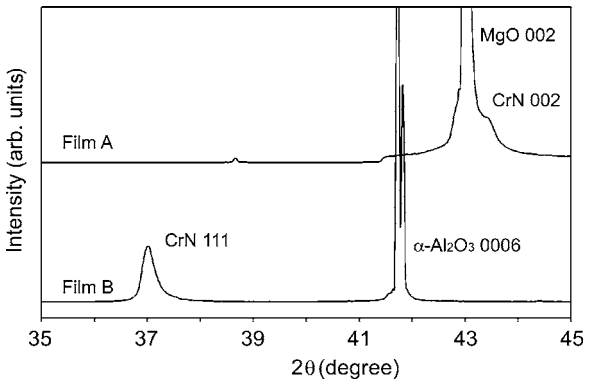

FIG. 2. Conventional ω-2θ scan x-ray diffraction patterns of CrN epitaxial films.

constants, the diffraction peaks associated with the crystal planes not parallel to the substrate surface were measured at room temperature using an x-ray diffractometer, equipped with a multiaxis sample stage. For films A and B, the 111, 200, 220, and 113 diffractions were measured at optimized positions, and the obtained d values were used to calculate the cell parameters, with the results listed in Table I. At room temperature, the lattice distortion of these CrN films from cubic symmetry was small. film A exhibited a small distortion from cubic to tetragonal symmetry, with expansion along the c axis ($c/a=1.010$), while film B only exhibited a very small trigonal distortion of $\alpha=89.32^{\circ}$.

Comparison between film B (thickness=68 nm) and film C (thickness=23 nm) gives information concerning the structural uniformity of the (111)-oriented CrN films. X-ray diffraction analysis gave very close cell parameters for the two films (only 0.2% difference). The data for film C represent the averaged structure for 23 nm thickness from the film/substrate interface. The small difference between films B and C indicates that the structure is uniform for these films (except very thin layers close to film/substrate interface).

The compositions of the films were determined by x-ray photoelectron spectroscopy. Bulk CrN of composition $Cr_1N_{0.956}$, as determined by EPMA analysis, was used as a standard to calibrate the x-ray photoelectron spectrometer.[23,24] The compositions of the films were measured to be $N/Cr=1.02\pm0.04$, 1.07 ± 0.04, and 1.08 ± 0.04 for films A, B, and C, respectively, showing that these films are almost stoichiometric.

In order to elucidate the lattice distortion behavior of the two CrN films, we carried out the temperature-controlled x-ray diffraction measurements of crystal planes parallel to the substrate surface (i.e., CrN 002 and CrN 111 for films A and B, respectively). Figure 3 shows the temperature dependence of these diffraction peaks. In Fig. 3(a), the CrN 002 peak of film A obviously shifted to a higher angle as the sample was cooled. On the other hand, the CrN 111 peaks in Fig. 3(b) had small shifts compared to those in Fig. 3(a).

Figure 4 shows the temperature dependence of the d values for the CrN (002) of film A (top panel) and the CrN (111) of film B (bottom panel). The ordinates represent relative d values compared to those at 290 K. For comparison, the d values for the diffraction from the substrates were also plotted in Fig. 4. The d values for MgO 002 monotonically decreased upon cooling. The thermal expansion coefficient of the MgO substrate was calculated to be 7.6×10^{-6} K^{-1} from the data between 125 and 290 K, being consistent with the literature (11.15×10^{-6} K^{-1} at 298 K).[26] The d values for CrN 002 in Fig. 4(a) obviously show a transition at 260–270 K, and this d value showed a steep decrease around the temperature when the sample was cooled. From the top panel of Fig. 4, the decrease in the d value of CrN 002 was estimated to be 0.27% from 290 to 150 K. From the reported lattice constants for bulk CrN, it was calculated that the 0.24% decrease in the d value of CrN 002 occurred when the

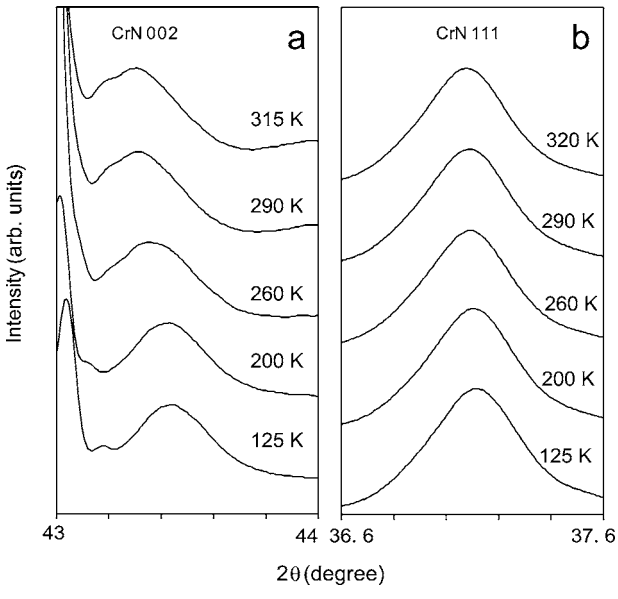

FIG. 3. Temperature-controlled x-ray diffraction patterns of CrN films. (a) CrN(001)/MgO(001) (film A); (b) CrN(111)/α-Al_2O_3(0001) (film B).

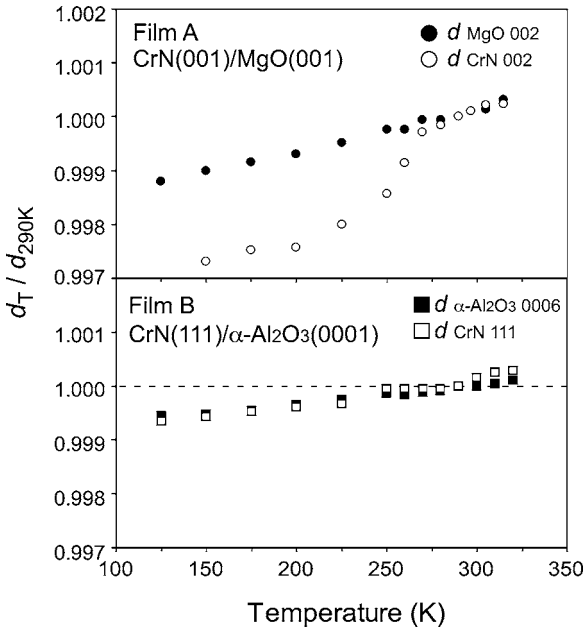

FIG. 4. Temperature dependences of d spacing of CrN films.

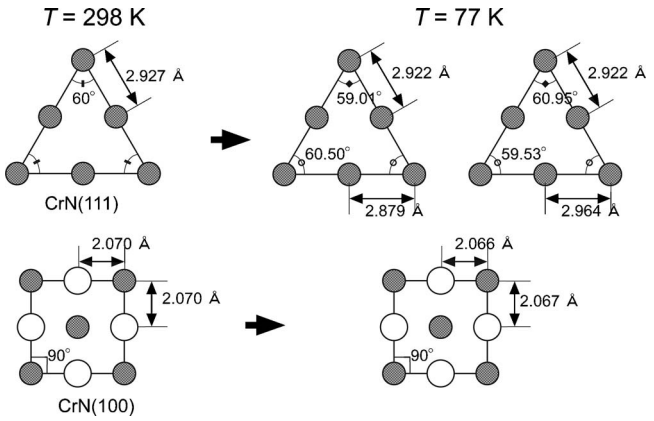

FIG. 5. Illustration of interatomic distances and bond angles calculated from reported bulk structure before and after the antiferromagnetic transition. Shaded circles: Cr; open circles: N.

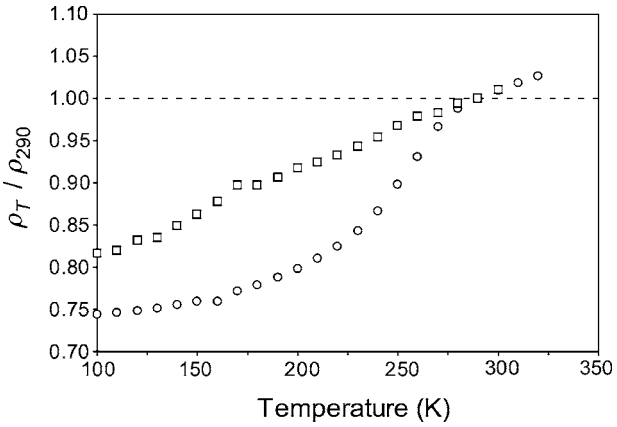

FIG. 6. Temperature dependence of resistivity of CrN films. Circles: CrN(001)/MgO(001) (film A), Squares: CrN(111)/α-Al_2O_3(0001) (film B).

sample was cooled from 298 to 77 K across the Néel temperature. The two values are close to each other, and we conclude therefore that the observed transition in the top panel of Fig. 4 is due to the lattice distortion accompanied by the antiferromagnetic transition of the CrN thin film.

On the other hand, as shown in the bottom panel of Fig. 4, the temperature dependence of the d values for the CrN 111 of film B was small, and no anomaly was observed except for a slight deviation at around 250 K from the linear dependence due to the thermal expansion of the CrN lattice. The antiferromagnetic transition of bulk CrN brings about a 1% change in the d value of CrN 111. We therefore concluded that the CrN (111) film grown on α-Al_2O_3(0001) did not show a structural transition due to antiferromagnetic ordering.

The above-mentioned results demonstrate that (001)-oriented CrN on MgO(001) showed a corresponding lattice distortion upon the antiferromagnetic transition, but (111)-oriented CrN on α-Al_2O_3(0001) did not show a transition. The different behaviors of the two films are explained in terms of changes in the interatomic distances on the film-substrate interfaces. Figure 5 schematically illustrates the changes in the interatomic distances and angles on the CrN (001) and CrN (111) crystal planes when the lattice distortion of the bulk CrN occurs. It is clear that the changes in the interatomic distances on CrN (001) are very small (around 0.1%) before and after the structural transition. On the other hand, significant changes are expected in the interatomic distances on CrN (111) due to the lattice distortion. Because of the lowering of the crystal structural symmetry from cubic to orthorhombic due to the change in α (Fig. 1), the two types of atom displacements are expected on CrN(111) planes: The Cr-Cr distance changes by a maximum of 1.6% on the Cr (111) plane (from 2.927 to 2.879 or 2.964 Å). In the case of the (111)-oriented CrN film on α-Al_2O_3(0001), the substrate fixes the positions of the atoms on the interface of CrN preventing them from changing their interatomic distances on CrN (111). Consequently, the lattice distortion of the film is suppressed for film B. Contrary to this, (001)-oriented CrN on MgO (001) is distorted without a large displacement of the atoms on the interface with the substrate.

The existence of structural transitions for the two film types were particularly influential on the electron transport properties of the films. Figure 6 represents the temperature dependence of the electronic conductivity of the films. The ordinate represents the relative values compared to those at 290 K. The CrN films on the substrates showed ρ values of 1.7×10^{-3} and 3.1×10^{-4} Ω cm for films A and B, respectively. These values are in the range of metallic conductors. Accordingly, film B showed metallic temperature dependence on ρ with no anomaly. Contrary to this, film A showed a steep decrease in its ρ value at around 250–270 K as the film was cooled. The temperature range is exactly the same as that of the lattice distortion observed for film A. In other words, film A showed a structural transition and a spontaneous steep decrease in its ρ value, while film B showed no structural transition and no anomaly in temperature dependence of its ρ value.

At present, it is not clear why the resistivity in film A decreases when the lattice distortion occurred. Some studies have reported different results for the electronic conductivity of (001)-oriented CrN grown on MgO(001). Smith *et al.*[17] reported that CrN grown on MgO(001) shows a transition from semiconductorlike behavior to metallic behavior when the film was cooled across the Néel temperature: The film showed a large and very steep decrease in its resistivity at the Néel temperature. Gall *et al.*[16] reported that CrN on MgO(001) is a semiconductor with an optical band gap of 0.7 eV. They observed no anomaly around the Néel point. As for the transport properties of bulk polycrystalline-CrN, Browne *et al.*[15] reported the observation of metallic behavior before and after the antiferromagnetic transition, accompanied by a steep decrease in resistivity when the sample was cooled across the Néel point. On the other hand, Herle *et al.*[14] reported that the bulk CrN polycrystalline sample exhibited semiconducting behavior.

As for the electronic conductivity of (001)-oriented CrN on MgO(001) (film A), our results are close to the report of Browne *et al.*[15] on bulk CrN: A steep change in its ρ value at the Néel temperature and metallic behavior at both sides of the Néel temperature. Our results are also similar to those of Smith *et al.*[17] in a sense that the ρ value shows a large

anomaly at the Néel point, and metallic conductivity below the Néel point. The reason for the differences between the studies is still unknown. Our results, however, clearly demonstrate that the steep change in electronic conductivity is caused by the lattice distortion and/or changes in the electronic structure closely related to the distortion. This is because the film without the lattice distortion did not show an anomaly in electronic conductivity.

Filippetti *et al.*[12,13] carried out detailed band calculations for CrN, both with and without the lattice distortion and antiferromagnetic ordering. The calculation predicted a very high density of states at the Fermi energy (E_F) in the paramagnetic state, and weak metal properties below the Néel point, where the antiferromagnetic ordering causes a large band splitting and the depletion (a pseudogap ~0.5 eV wide) in the DOS of a sharp region around E_F being a weak metal. Our results are consistent with the calculation in a sense that the films showed metallic conductivity.

Our present results highlight another interesting aspect of CrN epitaxial films. According to the calculation by Filippetti *et al.*[12,13] the double layer antiferromagnetic ordering is slightly favored over other single-layered antiferromagnetic ordering, due to the stabilization effect of the lattice distortion. We note that the suppression of the lattice distortion by epitaxy can theoretically bring about a destabilization of the known antiferromagnetic ordering (the alternating double layers), and stabilization of other magnetic states. We do not have direct data of magnetic properties of the films, because their magnetic responses were too small to measure with a magnetometer. A clue is the electronic conductivity (Fig. 6). No anomaly was observed in the electronic conductivity for the (111)-oriented CrN epitaxial film. This suggests that the paramagnetic states of CrN were maintained at temperature lower than the bulk-Néel point. This point is now under investigation.

CONCLUSIONS

Taking advantage of epitaxial growth, we found it was possible to control the existence of the structural transition of CrN films, further accompanied by the corresponding antiferromagnetic transition: Temperature controlled x-ray diffraction revealed that the distortion of the (111)-oriented CrN film on α-Al_2O_3(0001) was suppressed by the effect of epitaxy, while the (001)-oriented CrN film on MgO(001) showed a clear distortion under its Néel temperature. These films showed electron transport behaviors corresponding well to the presence and absence of the structural transition. Our present results highlight a possibility to control the electronic and/or magnetic properties of materials by preventing the occurrence of structural distortions that are observed for bulk samples, which will be an interesting subject for future studies.

ACKNOWLEDGMENTS

This work was partially supported by a COE project and a Grant-in-Aid for Scientific Research (A) and that on Priority Areas (No. 436) from the Japan Ministry of Education for Science, Culture, Sports and Technology (MEXT), and a CREST project from the Japan Science and Technology Corporation (JST).

[1] Y. Wakabayashi, D. Bizen, H. Nakao, Y. Murakami, M. Nakamura, Y. Ogimoto, K. Miyano, and H. Sawa, Phys. Rev. Lett. **96**, 017202 (2006).
[2] Y. Ogimoto, M. Nakamura, N. Takubo, H. Tamaru, M. Izumi, and K. Miyano, Phys. Rev. B **71**, 060403(R) (2005).
[3] M. Nakamura, Y. Ogimoto, H. Tamaru, N. Izumi, and K. Miyano, Appl. Phys. Lett. **86**, 182504 (2005).
[4] K. H. Ahn and A. J. Millis, Int. J. Mod. Phys. B **16**, 3281 (2002).
[5] P. Padhan and W. Prellier, Phys. Rev. B **72**, 094407 (2005).
[6] S. Dennler and J. Hafner, Phys. Rev. B **72**, 214413 (2005).
[7] J. Hafner and D. Spisak, Phys. Rev. B **72**, 144420 (2005).
[8] B. Heinrich, A. S. Arrott, C. Liu, and S. T. Purcell, J. Vac. Sci. Technol. A **5**, 1935 (1987).
[9] E. Kunnen, S. Mangin, V. V. Moshchalkov, Y. Bruynseraede, A. Hoser, and K. Temst, Thin Solid Films **414**, 262 (2002).
[10] S. Kusano, S. Nakatani, T. Takahashi, K. Hirano, S. Koh, M. Ebihara, T. Kondo, and R. Ito, Jpn. J. Appl. Phys., Part 1 **42**, 2582 (2003).
[11] L. M. Corliss, N. Elliot, and J. M. Hastings, Phys. Rev. **117**, 929 (1960).
[12] A. Filippetti, W. E. Pickett, and B. M. Klein, Phys. Rev. B **59**, 7043 (1999).
[13] A. Filippetti and N. A. Hill, Phys. Rev. Lett. **85**, 5166 (2000).
[14] P. S. Herle, M. S. Hedge, N. Y. Vasathacharya, S. Philip, M. V. R. Rao, and T. Sripathi, J. Solid State Chem. **134**, 120 (1997).
[15] J. D. Browne, P. R. Liddell, R. Street, and T. Millis, Phys. Status Solidi **1**, 715 (1970).
[16] D. Gall, C. S. Shin, R. T. Haasch, I. Petrov, and J. E. Greene, J. Appl. Phys. **91**, 5882 (2002).
[17] C. Constantin, M. B. Haider, D. Ingram, and A. R. Smith, Appl. Phys. Lett. **85**, 6371 (2004).
[18] K. Inumaru, T. Ohara, and S. Yamanaka, Appl. Surf. Sci. **158**, 375 (2000).
[19] K. Inumaru, H. Okamoto, and S. Yamanaka, J. Cryst. Growth **237**, 2050 (2002).
[20] K. Inumaru, T. Ohara, K. Tanaka, and S. Yamanaka, Appl. Surf. Sci. **235**, 460 (2004).
[21] K. Inumaru, Y. Kuroda, K. Sakamoto, M. Murashima, and S. Yamanaka, J. Alloys Compd. **372**, L1 (2004).
[22] K. Sakamoto, K. Inumaru, and S. Yamanaka, Appl. Surf. Sci. **199**, 303 (2002).
[23] K. Inumaru, K. Baba, and S. Yamanaka, Chem. Mater. **17**, 5935 (2005).
[24] K. Inumaru, K. Baba, and S. Yamanaka, Phys. Rev. B **73**, 052504 (2006).
[25] K. Inumaru, K. Baba, and S. Yamanaka, Physica B **383**, 84 (2006).
[26] T. R. Taylor, P. J. Hansen, B. Acikel, N. Pervez, R. A. York, S. K. Streiffer, and J. S. Speck, Appl. Phys. Lett. **80**, 1978 (2002).